DIRAC CONE AND TOPOLOGICAL STATES IN 2D PHONONIC CRYSTALS

ZAFER OZER[1], IZZAT AFANDIYEVA[2], AMIRULLAH M. MAMEDOV[3,4], EKMEL OZBAY[3]

[1]*Mersin Vocational High School Electronic and Automation Department, Mersin University, Turkiye*
[2]*Institute for Physical Problems Baku State University, Baku, Azerbaijan*
[3]*Nanotechnology Research Center (NANOTAM), Bilkent University, Turkiye*
[4]*International Scientific Center, Baku State University, Baku, Azerbaijan*
mamedov@bilkent.edu.tr

Dirac cones show many extraordinary properties, like phase reconstruction, topological edge state, and pseudo-diffusive behavior. A Dirac-cone-like dispersion at the center of the Brillouin zone where the wave number k = 0, is rare and only happens due to accidental degeneracy. At certain frequencies, the Dirac cone breaks the time-reversal symmetry of acoustic waves, which has not yet been fully explored. In present report, microarchitecture of phononic crystals (PnCs) in a periodic structure can be modulated to obtain the accidental triple degeneracies that make a Dirac-like cone at the k = 0. While doing so, it was observed that the frequency of a nondispersive "deaf" band obtained from any arbitrary periodic structure made of similar PnCs remains unaltered. Then, a deaf band based predictive modulation of the PnCs is realized, and multiple occurrences of the Dirac-like points are demonstrated. In addition, the Dirac cone frequency decreases gradually with increasing filling ratio, which indicates a possible way to control wave propagation on the subwavelength scale. Numerical simulation results show that acoustic metamaterials can behave like zero-refractive-index media and can be applied to acoustic tunnelling.

Keyword: double Dirac cone;topological edge state; rectangular phononic crystal;topological phase transition.
PACS: 43.30.+m;43.20.+g;42.70.Qs

1. INTRODUCTION

Acoustic metamaterials are periodic, semi-periodic or non-periodic artificial structures with acoustic properties not found in materials in nature. These materials have a wide variety of potential applications, including acoustic lens, [1-3], acoustic cloaking, [4,5] subwavelength resolution imaging [6–9], and acoustic super-tunneling, [10,11].

One of the reasons for band formation, which is the most important feature of acoustic metamaterials, is Bragg scattering that occurs in composite materials with different material densities and different elastic modulus [12–16].

Another reason for band formation is local resonance in acoustic metamaterials [17]. Locally resonant materials using a combination of high-density materials and soft coating materials can create band gaps with lattice constants two times smaller than the respective wavelength [17].

The most well-known locally resonant acoustic metamaterials, mass-spring systems [18–21], Helmholtz resonators [22–26], materials with Mie resonances [27,28] are stretched membranes [25,29–31].

Dirac cone structures showed many new extraordinary properties such as topological edge states [32-36], quantum Hall effect, [37,38]. Dirac cones in acoustic wave systems can be divided into three different categories: Dirac-like cone,[39] Dirac cone, [40-43] and double Dirac cone [44,45,47].

The first of these categories is the Dirac-like cone, which has triple degeneration of two linear distribution bands. A two-dimensional phononic crystal with a square lattice has been shown to have an effective zero mass density around the Dirac-like cone [39].

The second category is structures with a double degenerate Dirac cone located at the Brillouin region corner of the hexagonal or triangular lattice. [40–43] The third category is structures with double Dirac cones in the center of the Brillouin region [44–48].

In this study, the formation of sub-wavelength Dirac cones and the effect of the angle of the triangular resonators on the formation of Dirac cones in acoustic metamaterials consisting of circular, triangular and hexagonal Helmholtz resonators with hexagonal lattice were investigated using the finite element method.

2. MATERIAL AND METHODS

Phononic Crystal (PnC) consists of Helmholtz resonators made of different geometries BiTeI, BiTeCI and BiTeBr materials arranged in a triangular lattice shape in air. The elastic constant for BiTeBr is c_{44} =14.9 GPa, its density is 6760 kg/m^3, for BiTeI its elastic constant is c_{44} = 24.3 GPa, its density is 6869 kg/m^3, for BiTeCl its elastic constant c_{44} = 1.7 GPa and its density 6414 kg/m^3. According to the formula $\mathbf{c_{mat}} = \sqrt{\frac{c_{ij}}{\rho}}$, the formula of advance in the material was calculated as 1484 m/s for BiTeBr, 1881 m/s for BiTeI, and 514 m/s for BiTeCI respectively.

In Fig.1 for triangular inclusion b=26 mm, c=9.37 mm, w=1 mm, t=1 mm, for circular inclusion R=15 mm, w=1 mm, t=1 mm, for hexagonal inclusion 1 b=15 mm, c=7 mm, w=1mm t=1, mm and for hexagonal inclusion 2 b=18.85 mm, c=8.5 mm, w=1mm t=1, mm respectively.

131, H.Javid ave, AZ-1143, Baku
Institute of Physics
E-mail: jophphysics@gmail.com

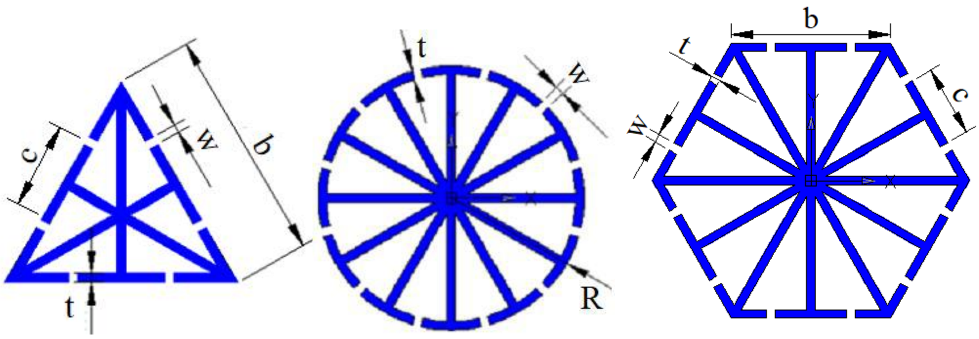

Fig. 1. Resonator sections and dimensions.

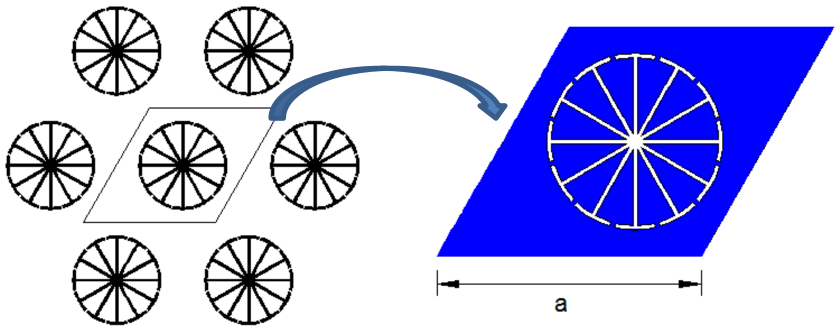

Fig. 2. Unit cell with triangular lattice.

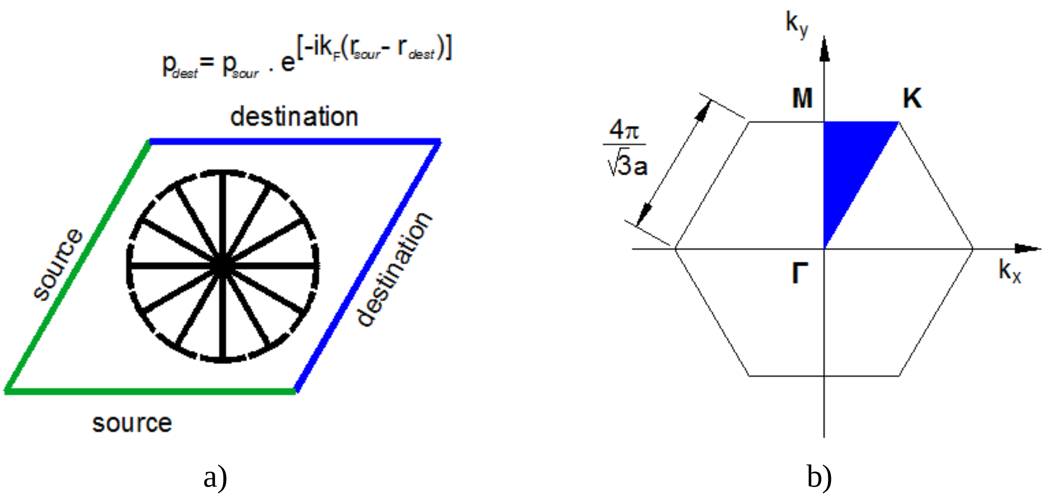

Fig. 3. a) Periodic boundary conditions applied to the unit cell b) 1. Brillouin zone of triangular lattice.

The geometry of the resonators is triangular, circular and hexagonal as shown in Fig.1.

The unit used to obtain the band structure of the triangular lattice PnC is as in Fig.2 and given for the circular resonator, the lattice constant is a=40 mm and other dimensions are as in Fig.1. To obtain the band structure, Floquet boundary conditions applied to the edges of the rhombic unit cell (Fig.3a). Fig.3b shows the 1st Brillouin region of the reciprocal lattice and the high symmetry

3. RESULTS AND ANALYSIS

We begin with the acoustic system that is shown in Fig. 4, which is a two-dimensional acoustic metamaterial that consists of a triangular array of regular columns with Helmholtz resonators. This acoustic metamaterial consists of six Helmholtz resonators. The first Brillouin zone of the triangular lattice is shown in Fig. 3, where the blue shading indicates the irreducible Brillouin zone.

Figure 4(a) shows that the dispersion relation becomes linear in the vicinity of the Dirac cone, which corresponds to the normalized frequency of 0.4346 (3727 Hz). For comparison, we also calculated the band structure of the complete triangular lattice with 90° rotation of resonant cavity, with results as shown in Fig. 4b. The phononic crystal has a Dirac cone at the normalized frequency of 0.4597 (3942 Hz). These results show that Helmholtz resonators can be used successfully to reduce the Dirac cone frequency. The introduction of acoustic metamaterials, therefore, offers the possibility that low-frequency Dirac cones can be obtained on a subwavelength scale.

To investigate the effects of the different space group symmetries on the Dirac cone, we discussed the unit cells with three different types of space group symmetry. As plotted in Fig. 2(a), the acoustic metamaterial with the space group symmetry p6 mm is arranged in a hexagonal lattice with a lattice constant a=40 mm. It should be noted that the gapless band structure has a Dirac cone at a normalized frequency of 0.2549 (2186 Hz). The band structure of the acoustic metamaterial with a rotation angle shows a Dirac cone at a normalized frequency of 0.2423 (1979 Hz). We observed that the Dirac cone frequency decreased after rotation; this reduction was induced by the spatial compression distribution after the rotation process. The angular dependence of the Dirac cone frequency is shown in Table 2 These results show the weak angular dependence of the Dirac cone frequency and indicate that when the acoustic metamaterial has the p6 mm space group symmetry, the Dirac cone remains robust to rotation.

We obtained the band structure when I rotate the triangular resonator 90° to the left is as follows. As seen in the picture, the band narrowed by 60% from the range of 0.4-0.55 (Fig.4a) to the range of 0.47-0.5 (Fig.4b).

Bands between 0.3514 and 0.3558 are formed in the circular resonator (Fig.5). A narrow band between 0.265-0.27 was formed in the hexagonal resonator (Fig.6).

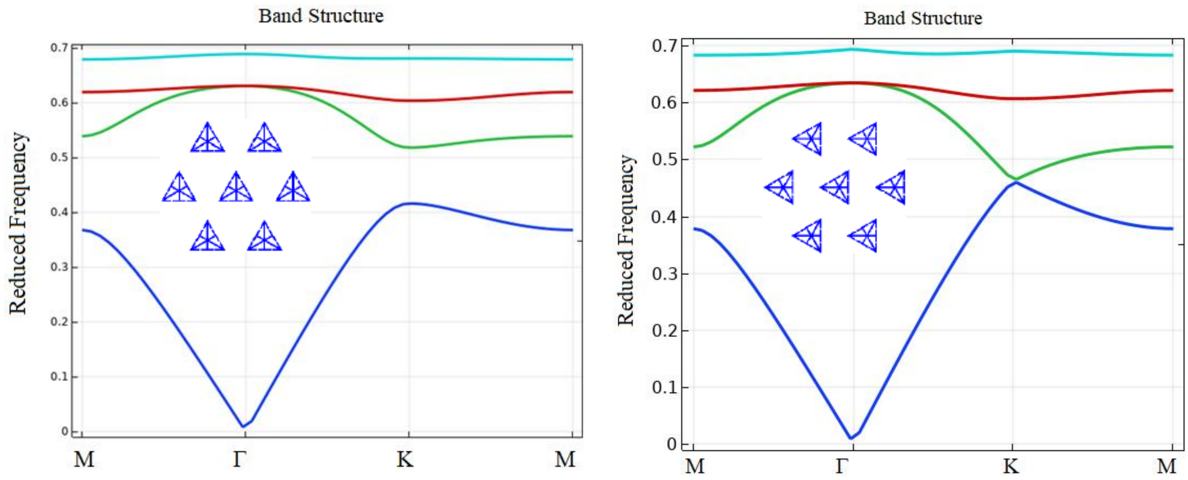

a) b)

Fig. 4. Band structure of BiTeI triangular resonator.

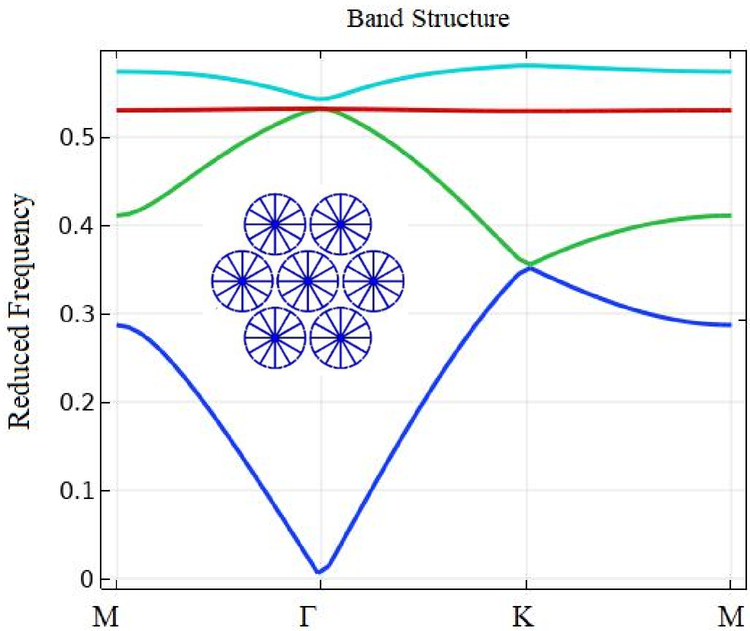

Fig. 5. Band structure of BiTeI circular resonator.

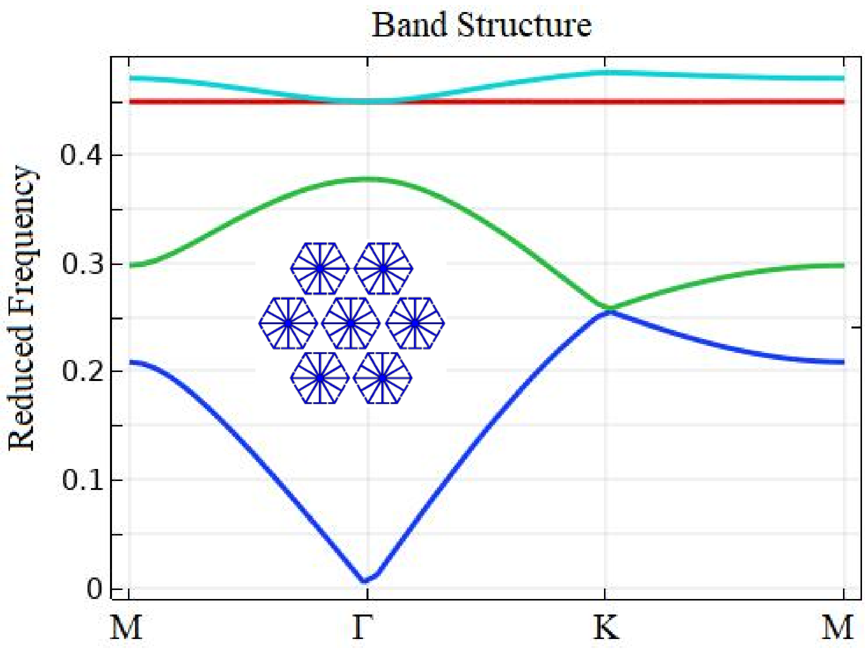

Fig. 6. Band structure of BiTeI hexagonal resonator.

Table 1.

Mid gap-gap size of different materials and cross-section of resonator.

	BiTeI		BiTeCI		BiTeBr	
	Mid Gap (a/c)	Gap Size (%)	Mid Gap (a/c)	Gap Size (%)	Mid Gap (a/c)	Gap Size (%)
Triangular resonator	0.475	31.579	0.395	1.113	0.468	20.771
90° rotated triangular resonator	0.485	6.186	-	-	-	-
Circular resonator	0.354	1.244	0.353	1.160	0.353	1.104
Hexagonal resonator	0.268	1.869	0.254	3.072	0.256	1.054

Table 1 shows the mid-gap, gap size values of the resonators in different sections made from BiTeI, BiTeCI and BiTeBr. As seen table 1 In the triangular resonator made of BiTeI, a band of 31.58% was observed in the range of 0.40-0.55, while a band of 6% was formed in the range of 0.47-0.50 when the resonator was rotated 90 degrees. While 1.2% band was formed in the range of 0.351-0.356 in the circular resonator, 2% band was formed in the range of 0.265-0.270 in the hexagonal resonator.

The resonator made of BiTeBr, a band of 1.11% was observed in the range of 0.393-0.397 in the triangular, 1.16% band was formed in the range of 0.351-0.356 in the circular resonator and 3% band was formed in the range of 0.250-0.258 in the hexagonal resonator.

The resonator made of BiTeCI, a band of 20.7% was observed in the range of 0.420-0.517 in the triangular, 1.1% band was formed in the range of 0.351-0.355 in the circular resonator and 1.05% band was formed in the range of 0.255-0.257 in the hexagonal resonator.

Table 2.

Dirac cone frequencies and normalized frequencies

	BiTeI		**BiTeCl**		**BiTeBr**	
	(Hz)	($f.a/c_0$)	(Hz)	($f.a/c_0$)	(Hz)	($f.a/c_0$)
Triangular resonator	3727	0.4346	3369	0.3929	3569	0.4162
Triangular (90° rotated) resonator	3942	0.4597	-	-	-	-
Circular resonator	3012	0.3513	3013	0.3514	3368	0.3928
Hexagonal resonator	2186	0.2549	2187	0.2551	2187	0.255

4. CONCLUSIONS

In this study, the band structure of PnCs consisting of Helmholtz resonators of different cross-sections with triangular lattice was obtained and the Dirac cone formation frequencies were investigated. Acoustic metamaterials composed of Helmholtz resonators enable Dirac cones to be obtained at the sub-wavelength scale. To investigate the effects of inclusions of different cross-sections on the Dirac cone, we created a unit cell in three different cross-sections, as shown in Fig. 2. Dirac cone frequencies in table 2 shows that rotation angle of inclusions affect the Dirac cone frequency.

[1] *S. Zhang, L. Yin and N. Fang*. 2009 Focusing Ultrasound with an Acoustic Metamaterial Network Phys. Rev. Lett. 102: 194301. https://doi.org/10.1103/PhysRevLett.102.194301

[2] *W. Wang, Y. Xie, A. Konneker, B.I. Popa and S.A. Cummer*. 2014 Design and demonstration of broadband thin planar diffractive acoustic lenses Appl. Phys. Lett. 105: 101904. https://doi.org/10.1063/1.4895619

[3] *N. Kaina, F. Lemoult, M. Fink and G. Lerosey*. 2015 Negative refractive index and acoustic superlens from multiple scattering in single negative metamaterial Nature 525: 77-81. https://doi.org/10.1038/nature14678

[4] *B.I. Popa, L. Zigoneanu and S.A. Cumme*. 2011 Experimental Acoustic Ground Cloak in Air Phys. Rev. Lett. 106: 253901. https://doi.org/10.1103/PhysRevLett.106.253901

[5] *X. Zhu, B. Liang, W. Kan, X. Zou and J. Cheng*. 2011 Acoustic Cloaking by a Superlens with Single-Negative Materials *Phys. Rev. Lett.* 106: 014301. https://doi.org/10.1103/PhysRevLett.106.014301

[6] *A. Sukhovich, B. Merheb, K. Muralidharan, J. Vasseur, Y. Pennec, P. Deymier and J. Page*. 2009 Experimental and Theoretical Evidence for Subwavelength Imaging in Phononic Crystals *Phys. Rev. Lett.* 102: 154301. https://doi.org/10.1103/PhysRevLett.102.154301

[7] *J. Zhu, J. Christensen, J. Jung, L. Martin-Moreno, X. Yin, L. Fok, X. Zhang and F. Garcia-Vidal*. 2011 A holey-structured metamaterial for acoustic deep-subwavelength imaging *Nat. Phys.* **7**: 52. https://doi.org/10.1038/nphys1804

[8] *J. Christensen and F.J.G. de Abajo*. 2012 Anisotropic Metamaterials for Full Control of Acoustic Waves *Phys. Rev. Lett*. 108: 124301. https://doi.org/10.1103/PhysRevLett.108.124301

[9] *M. Moleron and C. Daraio*. 2015 Acoustic metamaterial for subwavelength edge detection *Nat. Commun.* 6: 8037. doi: 10.1038/ncomms9037 (2015).

[10] *Z. Liang and J. Li*. 2012 Extreme Acoustic Metamaterial by Coiling Up Space *Phys. Rev. Lett.* 108: 114301. https://doi.org/10.1103/PhysRevLett.108.114301

[11] *Y. Cheng, C. Zhou, B.G. Yuan, D.J. Wu, Q. Wei and X.J. Liu*. 2015. Ultra-sparse metasurface for high reflection of low-frequency sound based on artificial Mie resonances *Nat. Mater.* 14: 1013. https://doi.org/10.1038/nmat4393

[12] *M.S. Kushwaha, P. Halevi, L. Dobrzynski, and B. Djafari-Rouhani*. 1993 Acoustic band structure of periodic elastic composites *Phys. Rev. Lett*. 71: 2022. https://doi.org/10.1103/PhysRevLett.71.2022

[13] *M.S. Kushwaha and P. Halevi*. 1994 Band-gap engineering in periodic elastic composites *Appl. Phys. Lett*. 64: 1085. https://doi.org/10.1063/1.110940

[14] *M.S. Kushwaha, P. Halevi, G. Martınez, L. Dobrzynski and B. DjafariRouhani*. 1994 Theory of acoustic band structure of periodic elastic composites Phys. Rev. B 49: 2313. https://doi.org/10.1103/PhysRevB.49.2313

[15] *Y. Pennec, J.O. Vasseur, B. Djafari-Rouhani, L. Dobrzynski and P.A Deymier*. 2010 Two-dimensional phononic crystals: Examples and applications Surf. Sci. Rep. 65: 229. https://doi.org/10.1016/j.surfrep.2010.08.002

[16] *L. Xie, B. Xia, J. Liu, G. Huang and J. Lei*. 2017 An improved fast plane wave expansion method for topology optimization of phononic crystals Int. J. Mech. Sci. 120: 171. https://doi.org/10.1016/j.ijmecsci.2016.11.023

[17] *Z. Liu, X. Zhang, Y. Mao, Y. Zhu, Z. Yang, C. Chan and P. Sheng*. 2000 Locally Resonant Sonic Materials Science 289: 1734. DOI: 10.1126/science.289.5485.1734

[18] *H.H. Huang and C.T. Sun*. 2009 Wave attenuation mechanism in an acoustic metamaterial with negative effective mass density New J. Phys. 11: 013003. https://doi.org/10.1088/1367-2630/11/1/013003

[19] *H.H. Huang and C.T. Sun*. 2011 Theoretical investigation of the behavior of an acoustic metamaterial with extreme Young's modulus J. Mech. Phys. Solids 59: 2070. https://doi.org/10.1016/j.jmps.2011.07.002

[20] *H.H. Huang and C.T. Sun*. 2012 Anomalous wave propagation in a one-dimensional acoustic metamaterial having simultaneously negative mass density and Young's modulus J. Acoust. Soc. Am. 132: 2887. https://doi.org/10.1121/1.4744977

[21] *S.H. Lee and O.B. Wright*. 2016 Anomalous wave propagation in a one-dimensional acoustic metamaterial having simultaneously negative mass density and Young's modulus Phys. Rev. B 93: 024302. https://doi.org/10.1121/1.4744977

[22] *N. Fang, D. Xi, J. Xu, M. Ambati, W. Srituravanich, C. Sun and X. Zhang*. 2006 Ultrasonic metamaterials with negative modulus *Nat. Mater*. **5**: 452. https://doi.org/10.1038/nmat1644

[23] *X. Hu, K.M. Ho, C. Chan and J. Zi*. 2008 Homogenization of acoustic metamaterials of Helmholtz resonators in fluid Phys. Rev. B 77:

172301. https://doi.org/10.1103/PhysRevB.77.172301

[24] *V. Garcia-Chocano, R. Gracia-Salgado, D. Torrent, F. Cervera and J. Sanchez-Dehesa.* 2012 Quasi-two-dimensional acoustic metamaterial with negative bulk modulus Phys. Rev. B 85: 184102. https://doi.org/10.1103/PhysRevB.85.184102

[25] *S.H. Lee, C.M. Park, Y.M Seo, Z.G. Wang and C.K. Kim.* 2010 Composite Acoustic Medium with Simultaneously Negative Density and Modulus Phys. Rev. Lett. 104: 054301. https://doi.org/10.1103/PhysRevLett.104.054301

[26] *B. Xia, Y. Qin, N. Chen, D. Yu and C. Jiang.* 2017. Dirac cones in two-dimensional acoustic metamaterials Sci. China: Technol. Sci. 60: 385. https://doi.org/10.1063/1.4998438

[27] *Y. Wu, Y. Lai and Z.Q. Zhang.* 2007. Effective medium theory for elastic metamaterials in two dimensions Phys. Rev. B 76: 205313. https://doi.org/10.1103/PhysRevB.76.205313

[28] *X. Zhou and G. Hu. 2009.* Analytic model of elastic metamaterials with local resonances Phys. Rev. B 79: 195109. https://doi.org/10.1103/PhysRevB.79.195109

[29] *Z. Yang, J. Mei, M. Yang, N. Chan and P. Sheng.* 2008 Membrane-Type Acoustic Metamaterial with Negative Dynamic Mass Phys. Rev. Lett. 101: 204301 (2008). https://doi.org/10.1103/PhysRevLett.101.204301

[30] *C.M. Park, J.J. Park, S.H. Lee, Y.M. Seo, C.K. Kim and S.H. Lee.* 2011 Amplification of Acoustic Evanescent Waves Using Metamaterial Slabs Phys. Rev. Lett. 107: 194301. https://doi.org/10.1103/PhysRevLett.107.194301

[31] *Y. Gu, Y. Cheng, J.S. Wang and X. J. Liu.* 2015 Controlling sound transmission with density-near-zero acoustic membrane network J. Appl. Phys. 118: 024505. https://doi.org/10.1063/1.4922669

[32] *S.R. Zandbergen and de M.J. Dood.* 2010 Experimental Observation of Strong Edge Effects on the Pseudodiffusive Transport of Light in Photonic Graphene Phys. Rev. Lett. 104: 043903. https://doi.org/10.1103/PhysRevLett.104.043903

[33] *Y.R. Poo, X. Wu, Z. Lin, Y. Yang and C.T. Chan.* 2011 Experimental Realization of Self-Guiding Unidirectional Electromagnetic Edge States Phys. Rev. Lett. 106: 093903. https://doi.org/10.1103/PhysRevLett.106.093903

[34] *P. Wang, L. Lu and K. Bertoldi.* 2015 Topological Phononic Crystals with One-Way Elastic Edge Waves Phys. Rev. Lett. 115: 104302. https://doi.org/10.1103/PhysRevLett.115.104302

[35] *Z. Yang, F. Gao, X. Shi, X. Lin, Z. Gao, Y. Chong and B. Zhang.* 2015 Topological Acoustics Phys. Rev. Lett. 114: 114301. https://doi.org/10.1103/PhysRevLett.114.114301

[36] *D. Torrent, D. Mayou and J. Sanchez-Dehesa.* 2013 Elastic analog of graphene: Dirac cones and edge states for flexural waves in thin plates Phys. Rev. B 87: 115143. https://doi.org/10.1103/PhysRevB.87.115143

[37] *K.S. Novoselov, A.K. Geim, S.V. Morozov, D. Jiang, Katsnelson M I, Grigorieva I.V, Dubonos S.V & A.A. Firsov.* 2005 Two-dimensional gas of massless Dirac fermions in graphene Nature 438: 197. https://doi.org/10.1038/nature04233

[38] *K.I. Bolotin, K.J. Sikes, Z. Jiang, M. Klima, G. Fudenberg, J. Hone, P. Kim and H.L. Stormer.* 2008 Ultrahigh electron mobility in suspended graphene Solid State Commun. 146: 351. https://doi.org/10.1016/j.ssc.2008.02.024

[39] *F. Liu, Y. Lai, X. Huang and C.T. Chan.* 2011 Dirac cones at k=0 in phononic crystals Phys. Rev. B 84, 224113. https://doi.org/10.1103/PhysRevB.84.224113

[40] *X. Zhang and Z. Liu.* 2008 Extremal Transmission and Beating Effect of Acoustic Waves in Two-Dimensional Sonic Crystals Phys. Rev. Lett. 101: 264303. https://doi.org/10.1103/PhysRevLett.101.264303

[41] *D. Malko, C. Neiss, F. Vines and A. Gorling.* 2012 Competition for Graphene: Graphynes with Direction-Dependent Dirac Cone Phys Rev Lett 108: 086804. https://doi.org/10.1103/PhysRevLett.108.086804

[42] *D. Torrent and J. Sanchez-Dehesa.* 2012 Acoustic Analogue of Graphene: Observation of Dirac Cones in Acoustic Surface Waves Phys Rev Lett 108: 174301 (2012). https://doi.org/10.1103/PhysRevLett.108.174301

[43] *J. Lu, C. Qiu, S. Xu, Y. Ye, M. Ke and Z. Liu.* 2014 Dirac cones in two-dimensional artificial crystals for classical waves Phys Rev B 89: 134302. https://doi.org/10.1103/PhysRevB.89.134302

[44] *Y. Li, Y. Wu and J. Mei.* 2014 Double Dirac cones in phononic crystals Appl Phys Lett 105: 014107. https://doi.org/10.1063/1.4890304

[45] *Y. Li and J.Mei.* 2015 Double Dirac cones in two-dimensional dielectric photonic crystals Opt Express 23: 12089. https://doi.org/10.1364/OE.23.012089

[46] *K. Sakoda.* 2012 Double Dirac cones in triangular-lattice metamaterials Opt Express 20: 9925. https://doi.org/10.1364/OE.20.009925

[47] *H. Dai, T. Liu, J. Jiao, B. Xia and D. Yu.* 2017 Double Dirac cone in two-dimensional phononic crystals beyond circular cells Journal of Applied Physics 121: 135105. https://doi.org/10.1063/1.4979852

[48] *Z.G. Chen, X. Ni, Y. Wu, C. He, X.C. Sun, L.Y. Zheng, M.H. Lu and Y.F. Chen.* 2014 Accidental degeneracy of double Dirac cones in a phononic crystal Sci Rep 4: 4613. DOI: 10.1038/srep04613